Comprehensive Assessment of Composition and Thermochemical Variability by High Resolution GC/QToF-MS and the Advanced Distillation-Curve Method as a Basis of Comparison for Reference Fuel Development*

Tara M. Lovestead[1], Jessica L. Burger[1], Nico Schneider[2], and Thomas J. Bruno[1]**

1) Applied Chemicals and Materials Division

National Institute of Standards and Technology

Boulder, CO

2) Ruhr-Universität Bochum, Germany

**Author to whom correspondence should be addressed: bruno@boulder.nist.gov

tel: 303-497-5158, fax: 303-497-6682

Abstract:

Commercial and military aviation is faced with challenges that include high fuel costs, undesirable emissions, and supply chain insecurity that result from the reliance on petroleum-based feedstocks. The development of alternative gas turbine fuels from renewable resources will likely be part of addressing these issues. The United States has established a target for one billion gallons of renewable fuels to enter the supply chain by 2018. These alternative fuels will have to be very similar in properties, chemistry, and composition to existing fuels. To further this goal, the National Jet Fuel Combustion Program (a collaboration of multiple U.S. agencies under the auspices of the Federal Aviation Administration, FAA) is coordinating measurements on three reference gas turbine fuels to be used as a basis of comparison. These fuels are reference fuels with certain properties that are at the limits of experience. These fuels include a low viscosity, low flash point, high hydrogen content "best case" JP-8 (POSF 10264) fuel, a relatively high viscosity, high flash point, low hydrogen content "worst case" JP-5 (POSF 10259) fuel, and a Jet-A (POSF 10325) fuel with relatively average properties. A comprehensive speciation of these fuels is provided in this paper by use of high resolution gas chromatography/quadrupole time-of-flight – mass spectrometry (GC/QToF-MS), which affords unprecedented resolution and exact molecular formula capabilities. The volatility information as derived from the measurement of the advanced distillation curve temperatures, T_k and T_h, provides an approximation of the vapor liquid equilibrium and examination of the composition channels provides detailed insight into thermochemical data. A comprehensive understanding of the compositional and thermophysical data of gas turbine fuels is required not only for comparison but also for modeling of such complex mixtures, which will, in turn, aid in the development of new fuels with the goals of diversified feedstocks, decreased pollution, and increased efficiency.

Keywords: advanced distillation curve, enthalpy, gas turbine fuel, GC/QToF-MS, and NMR

Introduction:

Present-day aviation is faced with challenges that include volatile fuel costs, undesirable emissions, and supply chain insecurity that result from the reliance on petroleum-based feedstocks. Both military and commercial gas turbine fuels are purchased under standard specifications that cover composition, volatility, fluidity, combustion, corrosion, thermal stability, contaminants, and additives.[1-3] Jet A is the most common commercial fuel available in the United States (U.S.).[2, 3] Jet A is similar to Jet A-1 (which is available outside the U.S. and has a lower freeze point) and is required to meet the specifications of ASTM-1655 for aviation turbine fuels.[2] JP-8 has been the major gas turbine fuel used by the U.S. military (MIL-DTL-83133).[1] JP-8 is Jet A-1 containing an additive package, which includes an icing inhibitor, corrosion inhibitor/lubricity enhancer, and anti-static additive.[3] JP-8 is replaced by JP-5 (MIL-DTL-5624) for shipboard use. JP-5 has a significantly higher flash point requirement than Jet A, Jet A-1, or JP-8, and is desirable from a safety standpoint.[4]

The development of alternative gas turbine fuels from renewable resources will likely be part of addressing these issues. The Federal Aviation Administration (FAA), for example, has established a target for one billion gallons of renewable fuels to enter the U.S. supply chain by 2018.[5] These alternative fuels will have to be very similar in properties, chemistry, and composition to existing fuels. For this reason, a solid understanding of which fuel properties are favorable and unfavorable is essential (both in fuel science and in the engineering community). To further this goal, the National Jet Fuel Combustion Program (a collaboration of multiple U.S. agencies under the auspices of the FAA) is coordinating measurements on three reference gas turbine fuels to be used as a basis of comparison. These fuels include a low viscosity, low flash point, high hydrogen content "best case" JP-8 fuel (POSF 10264), a relatively high viscosity, high flash point, low hydrogen content "worst case" JP-5 fuel (POSF 10289), and a Jet-A fuel with relatively average properties (POSF 10325).[6, 7] It should be noted that all of the mixtures meet specification,[2] but not all are optimal from an operational standpoint. A summary of the specification or fit-for-purpose properties of these three fuels is provided in Table 1.[6]

Proceeding from a philosophical viewpoint that fluid properties are derived from fluid composition, it follows logically that a more thorough and comprehensive knowledge of composition will form a better picture of fluid properties. Many methods have been developed to advance the chemical composition characterization of complex fluids (for example, fuels). These methods rely on analytical techniques such as gas chromatography (CG) with detectors including, mass spectrometry (MS), flame ionization detection (FID), electron capture detectors (ECD), sulfur chemiluminescence detectors (SCD), and/or thermal conductivity detectors (TCD), or nuclear magnetic resonance (NMR) spectroscopy.[8-11] More recently, advances in hyphenated GC-MS techniques have emerged including: GC-MS (ion-trap), GC time-of-flight (ToF), GC-MS triple quadrupole (QQQ), GC-ToF tandem MS, GC-QToF, and two dimensional GCxGC with either FID, MS or ToF-MS detection.[12] These techniques require sophisticated software packages and statistical analyses to elucidate the composition and relate this information to properties of complex fuels.[13-15] For fuels analyses, two dimensional GCxGC-ToF has been shown to have numerous advantages over traditional ASTM methods developed with GC-MS single quad including a very detailed picture of the chemical composition by chemical classification and carbon chain length. Advances in technology have also made possible high resolution GC/QToF-MS. GC/QToF-MS provides another avenue towards a better understanding of composition. GC/QToF-MS provides not only the exact mass of the molecules' radical cation, its molecular ion (typically the compounds molecular mass minus an electron). Thus, this method provides the exact molecular formula, but also, detailed deconvolution of the numerous overlapping peaks.

To probe the thermophysical properties of complex fuels, the volatility is often investigated by measurement of the distillation curves. The volatility is especially sensitive to even subtle changes in chemical composition, thus making the distillation curve very instructive. In earlier work, the method and apparatus for determining advanced distillation curves (ADCs) has been described and the resulting information has proven to be especially applicable to the characterization of complex fuels.[16-22] The ADC methodology offers significant improvements over previous approaches, such as ASTM D-86,[23] and can be applied to any complex or simple fluid mixture.

In this paper, a detailed chemical composition analysis of the aforementioned gas turbine research fuels: Jet A-10325, JP-8-10264, and JP-5-10289 is presented by use of high resolution GC/QToF-MS in order to better establish the link between chemical composition and thermophysical properties. These results are complemented by NMR analysis of the neat (undistilled) fuels, which provides insight into mole fractions of various classes of hydrocarbons. Moreover, the ADC methodology is used to enhance comparison of these three gas turbine fuels. Volatility information resulting from the measurements of the ADC-derived temperatures, T_k and T_h, provides an approximation of the vapor-liquid equilibrium. In addition, the examination of the ADC-derived composition channels gives detailed insight into the thermochemical properties of the fuels throughout the distillation, specifically the composite enthalpy of combustion. The data presented in this paper complements our earlier examination of the variability of gas turbine fuels, provides data necessary for the growing knowledge base, and is required to develop thermophysical models of complex mixtures.[24] These models will, in turn, aid in the development of novel fuels (or fuel blends) with *a priori* prediction of fuel properties, ultimately leading to the development of fuels from diversified feedstocks, that potentially decrease pollution, and are more efficient.

Experimental Section:

Materials: The gas turbine fuels used herein were provided by the Fuels Branch of the Air Force Research Laboratory (AFRL, Wright Patterson Air Force Base). Three jet fuels that have not been previously measured in our laboratory: Jet A-10325, JP-8-10264, and JP-5-10289 were analyzed along with one previously measured Jet A fuel, Jet A-4658.[24] This last fluid was a de-facto reference fuel that has been the basis for many measurements and model development studies. The jet fuels were used as is and housed in their original containers in a flammables cabinet without temperature control.

The solvent, acetone, obtained from a commercial supplier, was purity-checked by use of GC-MS and GC-FID. It was injected manually with a 10 μL gas-tight syringe into a split-splitless injector. The sample was vaporized in the injector port held at 280 °C with a constant head-pressure of 55.2 k·Pa (8 psig). The sample was separated on a 30 m capillary column (5 %-phenyl-95 %-dimethyl polysiloxane) with a film 0.25 μm thick. The column is housed in a

temperature-controlled oven that was 60 °C for four minutes, followed by a 20 °C / min increase to 300 °C at which point it remained at 300 °C for four minutes. FID and MS detection were used to quantify and identify any impurities. The MS detector recorded ions from 15 to 550 relative molecular mass (RMM). These spectra were analyzed manually with the aid of the NIST/EPA/NIH Mass Spectral Database released in 2011.[25, 26] This acetone was determined to be > 99 % (mass/mass), and thus, was used as is.

Analysis of Neat Fuels by GC/QToF-MS: GC/QToF-MS provides high sensitivity, selectivity and resolution with accurate mass, and thus, is able to provide detailed speciation of the neat (undistilled) jet fuels. A commercial instrument was used and analyses were performed in triplicate. Samples were prepared volumetrically by adding 2 μL of neat fuel into ~one mL acetone. An autosampler was used to inject 2 μL of each sample into the split/splitless injector with a split ratio of 50:1. A single taper liner with silanized pyrex wool was used. The injector was help at 280 °C and a constant column flow ultra-high purity He gas at 1 mL/min (initial head pressure was 48.95 kPa (7.1 psig)) was used. A fixed emission current of 35.0 μA and an electron energy of 70.0 eV were used. The samples were separated on a 30 m capillary column (5 %-phenyl-95 %-dimethyl polysiloxane) with a film 0.25 μm thick. The column, housed in a temperature-controlled oven, was programmed to be 40 °C for one minute and then to increase 10 °C / min to 260 °C. After exiting the GC column, the sample entered a quadrupole analyzer. The quadrupole analyzer parameters were set to allow all radical cations with a mass to charge ratio (m/z) from 45 to 750 amu to pass through to the collision cell. Typically, 1 mL/min nitrogen gas is purged into the collision cell as the quench gas. This gas is sufficient for the majority of tandem MS analyses in which only the precursor (parent) ion enters the collision cell to be fragmented into additional product ions. For fuels analyses, accurate identification of the hydrocarbons requires that the parent ions remain intact. In order to detect the parent ion of normal alkanes, the collision cell was modified to use helium (2 mL/min) as the quench gas. After exiting the collision cell, the sample entered a ToF analyzer. Ultimately, this extremely sensitive instrument provides the accurate mass of each compounds identified after deconvolution of the chromatogram, and thus, a detailed speciation with unprecedented accuracy was possible.

NMR Spectroscopy: Hydrocarbon Classification: A commercial 600 MHz NMR spectrometer with a cryoprobe, operated at 150.9 MHz for ^{13}C, was used to obtain quantitative ^{1}H and ^{13}C spectra.[27] For each fuel, three replicate ^{1}H and ^{13}C spectra were obtained. Samples for ^{1}H NMR spectroscopy were prepared by dissolving 10 µL of the fuel sample in 1 mL of acetone-D6; this NMR solvent contained 0.05 % of the chemical shift reference compound tetramethyl silane (TMS). Samples for ^{13}C NMR spectroscopy were prepared by mixing 0.5 mL of the fuel with 0.5 ml of chloroform-D; this NMR solvent contained 1.5 % by mass (0.06 M) of the relaxation agent chromium(III) acetylacetonate ($Cr(acac)_3$). Therefore, the final concentration of $Cr(acac)_3$ in the NMR sample was 0.03 M, which is comparable to concentrations conventionally used.[28] The samples were maintained at 25 °C for all of the NMR measurements. ^{1}H NMR spectra were referenced to the TMS peak at 0.0 ppm, and ^{13}C NMR spectra were referenced to the solvent peak at 77.0 ppm.

Quantitative ^{1}H NMR spectra were obtained with a 30° flip angle and a long interpulse delay (10.0 s acquisition time, 10.0 s relaxation delay). A sweep width of 12019.23 Hz (−4 ppm to 16 ppm) was used. After 64 scans the spectra had signal-to-noise ratios of about 2×10^4.

Quantitative ^{13}C spectra were obtained by use of inverse-gated waltz-16 proton decoupling and a relaxation agent (see above). An acquisition time of 0.909 s, a relaxation delay of 10.0 s, and a sweep width of 36057.69 Hz (−20 ppm to 220 ppm) were used. After 512 scans the spectra had signal-to-noise ratios of about 2000. The effectiveness of these parameters for producing quantitative ^{13}C spectra was verified previously by collecting spectra for three test compounds under similar conditions.[8]

For each neat fuel, ^{13}C DEPT-90 and ^{13}C DEPT-135 spectra were also obtained. For the DEPT experiments, a coupling constant ($J_{C\text{-}H}$) of 140 Hz was used, as recommended for hydrocarbon fuels with both aromatic and aliphatic components.[29] A sweep width of 29761.9 Hz (-10 ppm to 190 ppm) was used. Other acquisition parameters for the DEPT experiments included an acquisition time of 1.10 s, a relaxation delay of 2.0 s, and a total of 1024 scans. The DEPT spectra were used to determine the number of hydrogen atoms bonded to each type of carbon; that is, they were used to identify ^{13}C peaks, not to quantitate the different types of carbon.

ADC Methodology: The methods and procedure, advantages and numerous applications have been reported in previous works.[30-32] In brief, advanced distillation curves were performed at Boulder, Colorado's ambient atmospheric pressure (~83 kPa for the laboratory in Boulder, CO), which was recorded before and after each distillation by use of an electronic barometer that previously had been calibrated by use of a fixed cistern mercury barometer. This barometer was temperature corrected for the density of mercury and the brass scale expansion. Thus, the temperatures obtained could be adjusted to that which would be obtained at standard atmospheric pressure (1 atm = 101.325 kPa). This correction was based on the modified Sydney Young equation using a constant term that represents a fluid with an average carbon chain length of 12 (0.000109).[33-35]

Each distillation was with 200 mL of gas turbine fuel. Thermocouples (which had been previously calibrated in a fixed point cell) were used to record the boiling flask (kettle) temperature (T_k, the fluid temperature) and the head temperature (T_h, the temperature of the vapor at the bottom of the take-off position in the distillation head). Each temperature is important to record. T_k is a thermodynamically consistent temperature with which predictive models can be developed and T_h can approximate temperatures that might be obtained by use of ASTM D-86 (a classical distillation technique used by industry).[16, 17, 21, 22] In fact, head temperature measurements are always included in our distillation results table to allow quick and easy comparison with ASTM D-86 results. A model-predictive, programmable temperature controller was used to heat the boiling flask.[20] The temperature ramp program typically leads the distillation temperatures by ~60 °C without impacting the measured data. Vaporized fuel travels up through the distillation head (where T_h was measured), condenses in a vortex tube-cooled condenser,[16, 17] and passes through a receiver that was adapted with a hammock for the instantaneous sampling of the fuel distillate at predetermined distillate volume fractions (DVFs). A level-stabilized receiver, calibrated manually with Jet A-4658, was used to collect and measure the distillate volume.

Individual condensed vapor fractions (as they appear from the condenser at the receiver adapter hammock) were sampled and analyzed. A syringe was used to sample 7 μL of the distillate, which was then injected into pre-weighed autosampler vials containing known

amounts of acetone. The composition of each distillate volume fraction of fuel was studied by GC-MS and GC-FID with a 30 m capillary column of 5 % phenyl-95 % dimethyl polysiloxane, with a film thickness of 0.25 µm.[36] All samples were analyzed by the GC methods described above for acetone analysis. Peak identification was done manually and bny use of GC-MS with the NIST/EPA/NIH Mass Spectral Database released in 2011.[25, 26] GC-FID was used to quantify amounts of each compound. External calibration with n-octane was used in acetone.

Results and Discussion:

Analysis of the Neat Jet Fuels by GC/QTOF-MS: The chemical compositions of three jet fuels: Jet A-10325, JP-8-10264, and JP-5-10289, along with one previously measured fuel, Jet A-4658, were determined with high resolution GC/QToF-MS. For each neat fuel a chromatogram of the abundance of mass fragment ions as a function of acquisition time was collected. Figure 1 shows overlays of the chromatograms obtained for Jet A-10325 (red line), JP-8-10264 (blue line), and JP-5-10289 (green line). Figure 1 shows that JP-8-10264 has a greater abundance of "lights" (defined as compounds that elute before or with n-nonane, retention time, RT, = ~5.5 mins) when compared with the chromatograms obtained for Jet A-10325 and JP-5-10289. Figure 1 also shows that JP-5-10289 has a greater abundance of "heavy" (defined as compounds that elute after n-dodecane, RT = ~10 mins) compounds than the other two jet fuels examined. This observation is consistent with the specification or fit-for-purpose properties presented in Table 1. Interestingly, Figure 1 shows that more compounds elute after 14 mins from Jet A-10325 when compared with JP-8-10264 and JP-5-10289. This result is discussed in more detail when the compositional analysis presented in Table 2 is discussed.

The chromatograms obtained with high resolution GC/QToF-MS were analyzed with a commercial software package. First, a deconvolution algorithm resolved compounds that may have been obscured by the background noise of concurrently eluting compounds. Chromatogram deconvolution parameters were optimized using a surrogate of known compounds. Figure 2a shows the results of the deconvolution algorithm as applied to the Jet A-10325 chromatogram. Initially, over 170 compounds were resolved. A zoomed-in view of

the resolved compounds is shown in Figure 2b. Compounds were then identified manually, based on the species' radical cation's exact mass, and with guidance from the NIST/EPA/NIH Mass Spectral Database released in 2011. Figure 3 shows an example of a peak at 7.006 mins, identified as 1,3,5-trimethylbenzene. The GC/QToF-MS experimentally determined its radical cation's m/z to be 120.0934, which is the exact theoretical mass for this compound's radical cation.

Table 2 displays the most detailed list to date of the chemical compounds present in the neat Jet A-10325, JP-8-10264, and JP-5-10289 along with one previously measured fuel, Jet A-4658, by use of high resolution GC/QToF-MS. Table 2 presents all compounds identified listed with RT in mins, the Chemical Abstracts Service registry number (CAS No.), the chemical formula and RMM. If the substituent positions could not be determined these compounds are listed with x, y, or z, instead of specific position indexes or by their general chemical class, and in these instances a CAS No. is not provided.

Table 2 also presents the raw area percent relative to the total area of all of the compounds to aid in comparing each fuel side-by-side. A comprehensive uncertainty analysis of the raw area percent for hundreds of compounds is not practical. This would require calibrating the detector response for each compound in Table 2. Accurate area percent calculations also depend on the repeatability of the measured raw area percent, and uncertainty in compound identification. High resolution GC-QToF-MS provides the exact mass of the molecular formula with a high certainty in the chemical class identification. The calculated raw area percent uncertainty obtained from the deconvolutions of each chromatogram was examined with repeat injections. The raw area percents for the following three compounds: toluene (RT = 3.5 mins), n-undecane (RT = 8.7 mins) and n-pentadecane (RT = 14.2 mins) were determined to have an uncertainty of approximately 0.2 area percent. Thus, this methodology has good repeatability in raw area percent and high accuracy in determination of chemical compound or classification; therefore, the main contribution to uncertainty is in the calibration for chemical compound and the detector response. The area percent calculation, is only provided to examine the relative amounts of each compound. Providing this information is very valuable. Table 2 shows that each fuel is basically comprised of the same chemical

compounds just in differing amounts, thus it is imperative to have at least some basis for examining the relative concentrations of each compound.

Table 2 shows that JP-8-10264 has a greater relative percent of "lights" (12.1 %) compared to the other fuels: Jet A-10325 (6.0 %) and JP-5-10289 (2.5 %). Additionally, Table 2 presents that more than half (56.8 %) of JP-5-10289s compounds elute after n-dodecane (RT = approximately 10 mins) compared to only 39.1 % for Jet A-10325 and only 25.7 % for JP-8-10264. Also, Table 2 shows that Jet A-10325 has a greater raw area percent concentration of the higher carbon number n-alkanes: n-hexadecane and n-heptadecane. This fuel also has a much greater number and concentration of compounds that elute after n-pentadecane. This result is also shown graphically in Figure 1 and helps to explain the interesting behavior observed during the distillation of these fuels (which we will discuss in the following sections).

Hydrocarbon Classification by NMR Spectroscopy: NMR is useful to examine fuels because it gives an overview of carbon types needed for understanding of combustion properties of complex fuels like diesel and jet fuel.[13] NMR can also differentiate the amount of branching and highly-branched iso-paraffins burn quite differently than iso-paraffins with 1 or 2 branches.[6] Methods developed in other laboratories were used to determine the relative amounts of hydrogen and carbon bond types by spectral region integration..[13, 37, 38] For jet fuels, our laboratory has made some minor changes in how we report the integral regions. These methods have been reported previously.[8]

Four sources of uncertainty were considered for the peak integrals reported herein: incomplete relaxation and residual nuclear Overhauser effects (NOE), which are significant only for the ^{13}C NMR spectra, repeatability in the distillation, baseline drift, and temperature. The magnitude of the influence of these uncertainties has been assessed in the same manner as reported previously.[8] The estimated values for these sources of uncertainty were added in quadrature to arrive at the combined standard uncertainties that are reported.

Table 3 shows a comparison of the integral values for ^{1}H NMR spectral regions for the neat gas turbine fuels: Jet A-10325, JP-8-10264, and JP-5-10289. The integrals in Table 3 have not been corrected for the relative number of hydrogen atoms per carbon. That is, the integrals in Table 3 still reflect the fact that a paraffinic CH_3 group has three times the signal intensity that an aromatic CH will have. Another caveat for the data in Table 3 is the obvious lack of a category for paraffinic CH because peaks for this type of proton are not well separated from the other spectral regions. From the ^{13}C DEPT spectra, it is clear that paraffinic CH exists in all the jet fuels. The CH peaks are expected to be mostly subsumed into the large paraffinic CH_2 integral,[26] where their relative effect is minimized. They do, however, contribute significantly to the cycloparaffin region causing the amount of cycloparaffins to be overestimated.

Table 4 shows a comparison of the integral values for the ^{13}C NMR spectral regions for the neat gas turbine fuels: Jet A-10325, JP-8-10264, and JP-5-10289. The repeatability of the ^{13}C NMR measurement is not as good as the ^{1}H measurement because baseline drift is more important for the ^{13}C NMR spectra (which have relatively low signal-to-noise ratios), and there is some uncertainty due to relaxation and residual NOE effects. Consequently, the integral values for the ^{13}C NMR spectral regions have larger uncertainties. As one might suspect, the spectra for these sample were similar to what has been seen previously for jet fuels when analyzed by NMR.[8] The NMR tables present an extremely detailed view of the hydrogen and carbon bond types found in these three jet fuels. The best way to compare the aromatic content of each fuel is to examine Table 4 for the different mole percent of quaternary aromatics and aromatic CH. With our NMR method, only the aromatic carbon atoms (or aromatic hydrogen atoms) are included in the spectral region for aromatics; any other types of atoms found in the molecule are included in other spectral regions. Previous work has shown that the ^{13}C NMR analysis gives 6–8 % systematically lower values for the aromatic content of the fuel than the ^{1}H NMR analysis, presumably due to incomplete relaxation.

Initial Boiling Temperatures: Careful observation of each sample in the distillation flask during initial heating allowed determination of the onset of boiling for each fuel. The initial boiling behavior was established by recording the kettle temperature (T_k) at which bubbling

was sustained and the temperature at which the vapor rose into the distillation head. It has previously been demonstrated that this last temperature is the initial boiling temperature (IBT), i.e., an approximation of the bubble-point temperature at ambient pressure of the fuel.[39, 40] This measurement is noteworthy as it can be modeled with an equation of state, and is the only point at which the temperature, pressure, and liquid composition are known. Vapor-rise is accompanied by a sharp increase in T_h, and is, therefore, far less subjective to ascertain than the sustained bubbling temperature, and thus, is less uncertain. In fact, experience with previous mixtures indicates that the uncertainty in the sustained bubbling temperature is approximately 1 °C and the uncertainty in the vapor rise temperature is approximately 0.3 °C, as measured by T_k.[9-11]

In Table 5, the initial temperature observations for the fuel samples and the average measured atmospheric pressure for the duration of the distillation are presented. Both the sustained and vapor rise temperatures for JP-8-10264 are ~13 °C lower than those observed for Jet A-10325. Additionally, both the sustained bubbling and vapor rise temperatures for JP-5-10289 are more than 15 °C higher than those observed for Jet A-10325. These results are in agreement with the compositional data obtained with GC/QToF-MS. The differences in the initial temperatures were most likely due to the increased "lights" observed for JP-8-10264.

Distillation Curves: The temperature at both the kettle position and the head position were recorded throughout the measurement of the distillation curves, (T_k and T_h, respectively) at predetermined distillate volume fractions. The uncertainty in the thermodynamically significant temperature T_k was approximately 0.3 °C. The uncertainty in T_h was approximately 4.0 °C. The uncertainty in T_h is due to both the difficulty in placing the thermocouple in the exact same location in the distillation head and also from vapor condensation on the thermocouple during the distillation.

The uncertainty in the volume measurement that is used to obtain the distillate volume fraction was 0.05 mL in each case. Average kettle and head temperatures are reported for each distillate volume fraction for the gas turbine fuels Jet A-10325, JP-8-10264, and JP-5-10289 in Table 6, as well as, the average measured atmospheric pressure for the duration of the

distillation. These data, T_k as a function of distillate volume fraction, are also represented graphically in Figure 4.

The temperature at which the first drop of fluid falls into the lever stabilized is indicated as a tick mark on the temperature axis. The first drop is considered the 0.025 % distillate volume fraction. Distillation temperatures for JP-8-10264 were lower than those observed for both Jet A-10325 and JP-5-10289 throughout the entire distillation. Also, distillation temperatures observed for JP-5-10289 were higher than those observed for Jet A-10325 and JP-8-10264 throughout the entire distillation, except for at the 90 % distillate volume fraction, at which point Jet A-10325 boils at a higher temperature than JP-5-10289. This result is consistent with the results presented in both Table 2 and Figure 1. Jet A-10325 has a greater concentration of both n-hexadecane and n-heptadecane than the other new jet fuels. These higher carbon chain compounds require higher temperatures to vaporize out of the boiling fuel. Additionally, in order for JP-5-10289 to meet the aforementioned specification for a higher flash point, some of the light components are distilled off during formulation. Removing some of the lights requires concomitant removal of the higher boiling n-paraffins because they will crash out of solution without the solvating effects of the light compounds. Thus, an increased boiling temperature was observed for the lower distillate volume fractions and a decreased boiling temperature was observed for the higher distillate volume fractions.

While the measurement of T_h has no fundamental significance, the difference between the T_k and T_h measurement provides insight into the possibility of azeotropic behavior. Nothing indicative of azeotropy was observed for any of the jet fuels examined here.

To place the current distillation curve measurements into historical context, Figure 5 presents the distillation curves for the gas turbine fuels Jet A-10325, JP-8-10264, and JP-5-10289, in the context of the experimental base discussed by Burger et al.[24] Please see Ref. 13 for more details regarding these previously measured gas turbine fuels. The thin black lines represent these previously measured fuels, with Jet A-4658 denoted by the red square symbols. The shaded areas in blue and pink represent one and two standard deviations, respectively, from the average distillation temperatures of all 21 fuels measured in that earlier study.[24] The

standard deviation is used to describe the spread in the fuel's properties when obtained from different sources, not the experimental uncertainty. Figure 5 shows that Jet A-4658 vaporizes at slightly higher temperatures than Jet A-10325. Also, Figure 5 shows that JP-8-10264 vaporizes at slightly lower temperatures than the two standard deviation average of all of these fuels below ~ 25 % distillate volume fraction, at which point this fuel begins to approach the distillation behavior of Jet A-10325. Additionally, it is shown that JP-5-10289 vaporizes at the upper extreme of the two standard deviations of the average distillation temperatures until the ~ 30 % distillate volume fraction. At higher distillate volume fractions, this fuel's distillations temperatures converge to that of both the average and Jet A-10325.

GC-MS Hydrocarbon Classification: The analysis of distillate composition may be further enhanced by the use of a mass spectrometric classification technique, similar to ASTM D-2789, which gives the percent of the sample found in various hydrocarbon family types.[41, 42] The procedures, uncertainty, and the potential difficulties of this method have been reported previously.[21] In brief, this technique is specified for use in low olefinic gasoline, thus, this technique was not developed specifically for gas turbine fuels. This technique is useful because the fuel community has historically used ASTM D-2789 as a means with which to compare current and emerging jet fuels. Thus, it affords data for historical and consistent fuel comparisons with the experience base.

This analysis was applied to the gas turbine fuels, Jet A-10325, JP-8-10264, and JP-5-10289. Table 7 gives the percent of the hydrocarbon family type found in each neat fuel and Figure 6 shows the changes in the percent hydrocarbon family through the distillations of the gas turbine fuels. It is important to note that the sampling is done instantaneously and this compositional data is not cumulative; in fact, it is a snap-shot in time of the distillate. These analyses showed that the percent of indanes, tetralins and naphthalenes increases through the distillation in each jet fuel sample whereas the percent of alkyl benzenes decreases. This result is consistent with what we have always seen. These plots also show that JP-5-10289 has a greater percent composition of indanes, tetralins and dicycloparaffins throughout the distillation when compared to the other two fuels. Thus, it is possible that these compounds contribute to the increased boiling temperature of JP-5-10289, at least until the 90 % distillate

volume fraction. It is important to note that the ASTM D-2789 method may over count parrafinic material because branched compounds on a branched aromatic are all included in the paraffinic total.

Distillate Fraction Composition and Energy Content: Previous work has shown that the composition channel data from the distillation curve can be used to provide quantitative analysis on specific distillate fractions.[21, 22, 31, 43] One can obtain quantitative data by determining the composition of each distillate volume fraction, determining their mole fraction and calculating a composite enthalpy of combustion based on the enthalpy of combustion of individual (pure) components. The enthalpy of combustion of the major individual (pure) components is taken from a reliable database compilation.[44] Eight sources of uncertainty are taken into account in this calculation:[21, 22, 31] including (1) neglecting the enthalpy of mixing; (2) the uncertainty of each individual (pure component) enthalpy of combustion from the database; (3) the uncertainty in calculating the mole fraction; (4) the uncertainty from the inability to ascertain very closely related isomers; (5) the uncertainty associated by neglecting minor components; (6) the uncertainty from component misidentification; (7) the uncertainty introduced by poorly resolved eluting peaks; and (8) the uncertainty when experimental data for the pure component enthalpy of combustion are unavailable and the Cardozo equivalent chain model must be used.[44] These sources of uncertainty combine to an uncertainty of 5 % in the composite molar enthalpy calculations reported in this work. For the individual distillate volume fractions the uncertainty is greater for the earlier eluting fractions, with an estimated combined uncertainty of closer to 10 % for the initial drop.

Figure 7 shows the molar enthalpy of combustion as a function of the distillate volume fraction for each of the gas turbine fuel Jet A-10325, JP-8-10264, and JP-5-10289. For completeness, Figures S1 and S2 in the Supporting Information show the enthalpy data on a volume- and mass-basis, respectively. From an operational standpoint, volume-basis is most important and from an engineering standpoint, mass-basis is the most important. As stated above, a composite enthalpy of combustion is calculated based on the enthalpy of combustion of individual (pure) components of a distillate fraction, and the measured mole fractions of those

components. To convert to a mass-basis, each component's mole fraction is divided by the component's molecular mass prior to summation. The molar enthalpy of combustion increases throughout the distillation because the standard enthalpy of combustion for each individual component generally increases with molecular mass, and higher molecular mass species elute in greater mole fractions in later distillate volume fractions. To convert the molar-basis to a mass-basis, the mole fraction of each component is normalized by its molecular mass, thus decreasing the impact the higher molecular mass compounds on the composite enthalpy of combustion and no significant change is observed with increasing distillate volume fraction or compositional changes. To convert the mass-basis, the mole fraction of each component is multiplied by the density of each component. Since the density typically decreases with increasing molecular mass, once again, the impact the higher molecular mass compounds have on the composite enthalpy of combustion is decreased, and no change is observed with increasing distillate volume fraction or compositional changes.

The molar enthalpy of combustion (Table 8, Figure 7) increased with distillate volume fraction as the concentration of lighter compounds vaporized out of the fuel samples. Figure 7 and Table 8 reveal that, on a molar-basis JP-5-10289 has more energy content than the other two gas turbine fuels throughout the entire distillation. Figure 7 and Figures S1 and S2 and Table 8 and Tables S1 and S2 show that the changes in energy content of the distillate volume fractions for each fuel was only observed when the enthalpy of combustion on a molar-basis was examined. No differences were observed when comparing the data on a volume- or mass-basis within the calculated uncertainty.

Conclusions:

In this paper, a powerful technique for elucidating the chemical composition of complex fuels is presented and related to thermophysical properties measurement by use of the ADC method. This novel methodology was applied to three reference gas turbine fuels to be used as a basis of comparison for reference alternative fuel development. These fuels included Jet A-10325, JP-8-10264, and JP-5-10289. The chemical species of these gas turbine fuels were characterized by use of high resolution GC/QToF-MS. Additionally, these fuels were characterized by NMR and mole fractions of hydrocarbon classifications results presented

here are in good agreement with the trends reported earlier for jet fuels studies.[8, 24] The advanced distillation curve method was then used to link the compositional data with thermophysical measurements. The ADC method provided the volatility information. As expected the T_k of the distillation curves was the highest for JP-5-10289 at all distillate volume fractions except for 90 %, and Jet A-10325 boiled at greater temperature than JP-8-10264 throughout the distillation. The ADC method also provided an explicit measure of the energy content of each distillate volume fraction. The molar enthalpy of combustion was observed to increase with distillate volume fraction as the concentration of lighter compounds vaporized out of the fuel samples and, on a molar-basis, JP-5-10289 has more energy content than the other two gas turbine fuels throughout the distillation range investigated. More work is necessary to determine the limitations of the numerous methodologies available, including high resolution GC/QToF-MS which was employed herein. The results will aid novel fuels to be compared with fuels currently in the supply chain. In addition, the data collected here adds to the growing understanding of the thermophysical property data of gas turbine fuels, which is required for thermophysical property modeling systems. Such modeling will, in turn, aid in the development of new fuels and optimization of engines with the goals of diversify feedstocks, decreasing pollution, and increasing efficiency.

Acknowlegements:

JB acknowledges the support of the Professional Research Experience Program (PREP) program for postdoctoral research. NS acknowledges Germany's Excellence Initiative [DFG GSC 98/3] and the Ruhr University Research School PLUS.

References:

(1) Mayfield, H. T. *JP-8 Composition and Variability*; DTIC Document: 1996.

(2) D1655-15d, A. S., Standard Specification for Aviation Turbine Fuels. In ASTM International, West Conshohocken, PA: 2011. www.astm.org

(3) Verevkin, S. P.; Emel'yaneriko, V. N., Transpiration method: Vapor pressures and enthalpies of vaporization of some low-boiling esters. *Fluid Phase Equilib.* **2008**, 266(1-2), 64-75.

(4) Martel, C. R. *Military Jet Fuels, 1944-1987*; Rept. AFWAL-TR-87-2062, Air Force Wright Aeronautical Laboratory, 1987.

(5) *National Aeronautics Research and Development Plan*; Executive Office of the President, National Science and Technology Council: Washington, D.C. 20502, February 2010.

(6) Edwards, J. T., Personal Communication. In 2016. james.edwards.17@us.af.mil

(7) Colket, M.; Heyne, J.; Rumizen, M.; Gupta, M.; Jardines, A.; Edwards, T.; Roquemore, W.; Andac, G.; Boehm, R.; Zelina, J.; Lovett, J.; Condevaux, J.; Bornstein, S.; Rizk, N.; Turner, D.; Graves, C.; Anand, M. S., An Overview of the National Jet Fuels Combustion Program. *AIAA* **2016**, 2016-0177.

(8) Burger, J. L.; Widegren, J.; Lovestead, T. M.; Bruno, T. J., 1H and 13C NMR Analysis of Gas Turbine Fuels as Applied to the Advanced Distillation Curve Method. *Energy and Fuels* **2015**, 29(8), 4874-85.

(9) Bruno, T. J.; Ott, L. S.; Smith, B. L.; Lovestead, T. M., Complex fluid analysis with the advanced distillation curve approach. *Anal. Chem.* **2010**, 82, 777-83.

(10) Bruno, T. J.; Ott, L. S.; Lovestead, T. M.; Huber, M. L., Relating complex fluid composition and thermophysical properties with the advanced distillation curve approach. *Chemical Eng. Tech.* **2010**, 33(3), 363-76.

(11) Bruno, T. J., Ott, L.S., Lovestead, T.M., Huber, M.L., The composition explicit distillation curve technique: relating chemical analysis and physical properties of complex fluids. *J. Chromatogr.* **2010**, A1217, 2703-15.

(12) Bruno, T. J., *CRC Handbook of Chemistry and Physics, 97th ed.* Taylor and Francis CRC Press: Boca Raton, 2016-2017.

(13) Mueller, C. J.; Cannella, W. J.; Bays, J. T.; Bruno, T. J.; DeFabio, K.; Dettman, H. D.; Gieleciak, R. M.; Huber, M. L.; Kweon, C.-B.; McConnell, S. S.; Pitz, W. J.; Ratcliff, M. A., Diesel surrogate fuels for engine testing and chemical-kinetic modeling: Compositions and properties. *Energy & Fuels* **2016**, 30, 1445-61.

(14) Kehimkar, B.; Parsons, B. A.; Hoggard, J. C.; Billingsley, M. C.; Bruno, T. J.; Synovec, R. E., Modeling RP-1 fuel advanced distillation data using comprehensive two-dimensional gas chromatography coupled with time-of-flight mass spectrometry and partial least squares analysis. *Anal. Bioanal. Chem.* **2015**, 407, 321-30.

(15) Kehimkar, B.; Hoggard, J. C.; Marney, L. C.; Billingsley, M. C.; Fraga, C. G.; Bruno, T. J.; Synovec, R. E., Correlation of rocket propulsion fuel properties with chemical composition using comprehensive two-dimensional gas chromatography with time-of-flight mass spectrometry followed by partial elast squares regression analysis. *Journal of Chromatography A* **2014**, 1327, 132-40.

(16) Bruno, T. J., Improvements in the measurement of distillation curves - part 1: a composition-explicit approach. *Ind. Eng. Chem. Res.* **2006**, 45, 4371-80.

(17) Bruno, T. J., Smith, B. L., Improvements in the measurement of distillation curves - part 2: application to aerospace/aviation fuels RP-1 and S-8. *Ind. Eng. Chem. Res.* **2006**, 45, 4381-88.
(18) Ott, L. S.; Bruno, T. J., Corrosivity of fluids as a function of distillate cut: application of an advanced distillation curve method. *Energy and Fuels* **2007**, 21, 2778 - 84.
(19) Ott, L. S., Bruno, T. J., Modifications to the copper strip corrosion test for the measurement of microscale samples. *J. Sulfur Chem.* **2007**, 28(5), 493 - 504.
(20) Smith, B. L.; Bruno, T. J., Advanced distillation curve measurement with a model predictive temperature controller. *Int. J. Thermophys.* **2006**, 27, 1419-34.
(21) Smith, B. L., Bruno, T. J., Improvements in the measurement of distillation curves: part 3 - application to gasoline and gasoline + methanol mixtures. *Ind. Eng. Chem. Res.* **2007**, 46, 297-309.
(22) Smith, B. L., Bruno, T. J., Improvements in the measurement of distillation curves: part 4- application to the aviation turbine fuel Jet-A. *Ind. Eng. Chem. Res.* **2007**, 46, 310-20.
(23) *Standard Test Method for Distillation of Petroleum Products at Atmospheric Pressure, ASTM Standard D 86-04b, Book of Standards Volume: 05.01*. American Society for Testing and Materials: West Conshohocken, PA, 2004.
(24) Burger, J. L.; Bruno, T. J., Application of the Advanced Distillation Curve Method to the Variability of Jet Fuels. *Energy & Fuels* **2012**, 26(6), 3661-71.
(25) NIST/EPA/NIH Mass Spectral Database, S. R. D., 2011. SRD Program, National Institute of Standards and Technology, Gaithersburg, MD.
(26) Bruno, T. J., Svoronos, P. D. N., *CRC Handbook of Basic Tables for Chemical Analysis, 3rd. ed.* . Taylor and Francis CRC Press: Boca Raton, 2011.
(27) Schoolery, J. N., Some quantitative applications of 13C NMR spectroscopy. *Progress in Nullear Magnetic Resonance Spectrometry* **1997**, 11, 79 - 93.
(28) Zhou, Z.; He, Y.; Qiu, X.; Redwine, D.; Potter, J.; Cong, R.; Miller, M. In *Optimum Cr (acac) 3 Concentration for NMR Quantitative Analysis of Polyolefins*, Macromolecular Symposia, 2013; Wiley Online Library: pp 115-22.
(29) Petrakis, L.; Allen, D., *NMR for Liquid Fossil Fuels*. Elsevier: 1986.
(30) Bruno, T. J.; Smith, B. L., Enthalpy of combustion of fuels as a function of distillate cut: application of an advanced distillation curve method. *Energy & Fuels* **2006**, 20, 2109-16.
(31) Bruno, T. J., Method and apparatus for precision in-line sampling of distillate. *Sep. Sci. Technol.* **2006**, 41(2), 309-14.
(32) Ott, L. S.; Smith, B. L.; Bruno, T. J., Experimental test of the Sydney Young equation for the presentation of distillation curves. *J. Chem. Thermodynam.* **2008**, 40, 1352-57.
(33) Young, S., Correction of boiling points of liquids from observed to normal pressures. *Proc. Chem. Soc.* **1902**, 81, 777.
(34) Young, S., *Fractional distillation*. Macmillan and Co., Ltd.: London, 1903.
(35) Young, S., *Distillation principles and processes*. Macmillan and Co., Ltd.: London, 1922.
(36) Windom, B. C., Lovestead, T. M., Riggs, J. R., Nickell, C., Bruno, T. J., Assessment of the compositional variability of RP-1 and RP-2 with the advanced distillation

curve approach. In *Proceedings of the 57th JANNAF Conference, Colorado Springs, CO (May, 2010)*, 2010.
(37) Japanwala, S.; Chung, K. H.; Dettman, H. D.; Gray, M. G., Quality of Distillates from Repeated Recycle of Residue. *Energy and Fuels* **2002**, 16(2), 477-84.
(38) Zigler, B. T., Fuels for Advanced Combustion Engines. In Laboratory, N. R. E., Ed. 2012.
(39) Bruno, T. J., Smith, B. L., Evaluation of the physicochemical authenticity of aviation kerosene surrogate mixtures Part I: Analysis of volatility with the advanced distillation curve *Energy & Fuels* **2010**, 24, 4266-76.
(40) Bruno, T. J.; Huber, M. L., Evaluation of the physicochemical authenticity of aviation kerosene surrogate mixtures Part II: Analysis and prediction of thermophysical properties. *Energy & Fuels* **2010**, 24, 4277-84.
(41) Gong, Y. F.; Liu, S. H.; Guo, H. J.; Hu, T. G.; Zhou, L. B., A new diesel oxygenate additive and its effects on engine combustion and emissions. *Applied Thermal Engineering* **2007**, 27(1), 202-07.
(42) Shafer, L. M.; Striebich, R. C.; Gomach, J.; Edwards, T. In *Chemical class composition of commercial jet fuels and other specialty kerosene fuels*, 14th AIAA/AHI Space Planes and Hypersonic Systems and Technologies Conference, paper 7972, Reno, NV, 2006; American Institute of Aeronautics and Astronautics: pp 1-6.
(43) Windom, B. C.; Lovestead, T. M.; Mascal, M.; Nikitin, E. B.; Bruno, T. J., Advanced distillation curve analysis on ethyl levulinate as a diesel fuel oxygenate and a hybrid biodiesel fuel. *Energy & Fuels* **2011**, 25(4), 1878-90.
(44) Rowley, R. L.; Wilding, W. V.; Oscarson, J. L.; Zundel, N. A.; Marshall, T. L.; Daubert, T. E.; Danner, R. P., *DIPPR(R) Data Compilation of Pure Compound Properties*. Design Institute for Physical Properties, A.: New York, Sept 2008.

Table 1. A summary of the specification or fit-for-purpose properties of the representative gas turbine fuels studied. The uncertainties are consistent with the uncertainty and bias statements of the individual standard and method.[6]

Property	**ASTM Method**	**Jet A**	**JP-5**	**JP-8**
Density @ 15 °C (g/mL)	ASTM D 4052-11	0.803	0.827	0.780
Kinematic Viscosity @ -20 °C (mm^2/s)	ASTM D 445-12	4.5	6.5	3.5
Flash Point (°C)	ASTM D 93-05	48	60	42
Freezing Point (°C)	ASTM D 5972-05	-52	-50	-51
Net Heat of Combustion (MJ/kg)	ASTM D 4809-13	43.0	43.0	43.1
Derived Cetane Number	ASTM D 6890	48.3	39.2	48.8
Aromatics (% (vol/vol))	ASTM D 1319-13	17.0	18.3	11.2
Hydrogen Content (% (mass/mass) by NMR)	ASTM D 7171-05	13.9	13.4	14.4

Table 2. A comparison of the raw area percent relative to the total area of all of the compounds for each of the neat gas turbine fuels, Jet A-10325, JP-8-10264, and JP-5-10289 along with one previously measured fuel, Jet A-4658[24]. The fuels were analyzed by use of GC/QTOF-MS as described above. A listing of all compounds, retention times (RTs) in mins, the Chemical Abstracts Service registry number (CAS No.), the chemical formula, and the relative molecular mass (RMM) are presented. There are several instances in which the substituent positions could not be determined on the basis of the mass spectrum, these compounds are listed with x, y, or z, instead of the position index or, by their general chemical class, and in these instances a CAS No. is not provided.

RT	Compound Name	CAS No.	Formula	RMM	Jet A-4658	Jet A-10325	JP-8-10264	JP-5-10289
(Mins)				(amu)	(area %)	(area %)	(area %)	(area %)
2.40	benzene	71-43-2	C_6H_6	78.05	tr	tr	0.1	tr
2.69	n-heptane	142-82-5	C_7H_{16}	100.13	tr	tr	0.1	
2.96	cyclohexane, methyl	108-87-2	C_7H_{14}	98.11	0.1	0.2	0.4	tr
3.45	heptane, 2-methyl	592-27-8	C_8H_{18}	114.14	0.1		0.2	
3.51	toluene	108-88-3	C_7H_8	92.06	0.3	0.3	0.4	0.1
3.55	heptane, 3-methyl-	589-81-1	C_8H_{18}	114.14			0.2	
3.64	cyclohexane, 1,3-dimethyl-, cis-	638-04-0	C_9H_{18}	112.13		0.3	0.5	
3.92	n-octane	111-65-9	C_8H_{18}	114.14	0.3	0.3	0.8	0.1
4.02	cyclohexane, 1,x-dimethyl-		C_8H_{16}	112.13			0.1	
4.24	heptane, 2,x-dimethyl-		C_9H_{20}	128.16		tr	0.1	
4.34	heptane, 2,x-dimethyl-		C_9H_{20}	128.16	0.1	0.1	0.2	
4.44	cyclohexane, ethyl-	1678-91-7	C_8H_{16}	112.13	0.2	0.3	0.6	0.2
4.48	cyclohexane, 1,1,3-trimethyl-	3073-66-3	C_9H_{18}	126.14		0.2	0.3	0.2
4.58							0.1	
4.71	cyclohexane, 1,x,y-trimethyl-		C_9H_{18}	126.14	0.2	0.2	0.2	0.1
4.78	C9-monocycloparaffin		C_9H_{18}	126.14		0.1	0.2	
4.88	octane, 4-methyl	2216-34-4	C_9H_{20}	128.16	0.4	0.4	0.6	0.2
5.00	p-xylene	106-42-3	C_8H_{10}	106.08	1.0	1.6	2.9	0.5

5.22	cyclohexane, 1,x,y,z-tetramethyl-		$C_{10}H_{20}$	140.16			0.2	
5.28	1-ethyl-x-methylcyclohexane (c,t)		C_9H_{18}	126.14	0.1	0.3	0.5	0.3
5.31	1-ethyl-x-methylcyclohexane (c,t)		C_9H_{18}	126.14			0.2	
5.37	o-xylene	95-47-6	C_8H_{10}	106.08	0.5	0.7	0.7	0.3
5.41	n-nonane	111-84-2	C_9H_{20}	128.16	0.6	0.8	2.6	0.4
5.55	C9-monocycloparaffin		C_9H_{18}	126.14			0.2	
5.59	1-ethyl-x-methylcyclohexane (c,t)		C_9H_{18}	126.14	0.2	0.3	0.3	0.2
5.64	C9-monocycloparaffin		C_9H_{18}	126.14			0.2	
5.74	heptane, 2,4,6-trimethyl-	2613-61-8	$C_{10}H_{22}$	142.17		0.1	0.3	
5.80	1H-indene, octahydro-	4551-51-3	C_9H_{16}	124.13	0.2	0.3	0.3	0.3
5.85	C10-monocycloparaffin		$C_{10}H_{20}$	140.16			0.5	
5.88	alkyl benzene		C_9H_{12}	120.09	0.3	0.3		0.2
5.92	C9-dicycloparaffin		C_9H_{16}	124.13			0.3	
5.96	cyclohexane, propyl	1678-92-8	C_9H_{18}	126.14	0.3	0.6	0.9	0.3
6.00	paraffin		$C_{10}H_{22}$	142.17	0.3	0.3	1.2	
6.10	monocycloparaffin		$C_{10}H_{20}$	140.16	0.3	0.4	0.4	
6.12	C10-monocycloparaffin		$C_{10}H_{20}$	140.16	0.3	0.4		
6.15	C10-monocycloparaffin		$C_{10}H_{20}$	140.16				0.2
6.24	C10-moncycloparaffin		$C_{10}H_{20}$	140.16	0.1	0.2	0.2	0.1
6.36	benzene, propyl-	103-65-1	C_9H_{12}	120.09	0.3	0.4	0.9	0.3
6.40	C10-monocycloparaffin		$C_{10}H_{20}$	140.16	0.4	0.4	0.3	0.2
6.43	C10-paraffin		$C_{10}H_{22}$	142.17			0.4	
6.45	C10-paraffin		$C_{10}H_{22}$	142.17	0.4	0.6	1.3	
6.49	alkyl benzene		C_9H_{12}	120.09	1.2	1.3	2.8	0.7
6.56	C10-parrafin		$C_{10}H_{22}$	142.17	0.4		0.2	
6.60	mesitylene	108-67-8	C_9H_{12}	120.09	0.9	1.5	3.1	0.5
6.67	C10-monocycloparaffin		$C_{10}H_{20}$	140.16	0.3	0.4	0.4	0.3

6.71	C10-dicycloparaffin		$C_{10}H_{18}$	138.14		0.3	0.4	
6.79	benzene, 1-ethyl-2-methyl-	611-14-3	C_9H_{12}	120.09	0.5	0.6	0.3	0.3
6.82	C10-monocycloparaffin		$C_{10}H_{20}$	140.16	0.5	0.6	0.7	0.4
6.87	C10-monocycloparaffin		$C_{10}H_{20}$	140.16	0.3	0.5	0.6	
6.96	alkyl benzene		$C_{10}H_{14}$	134.11	2.2	3.8	3.2	1.3
7.03	n-decane	124-18-5	$C_{10}H_{22}$	142.17	1.4	1.7	6.1	0.9
7.19	C10-monocycloparaffin		$C_{10}H_{20}$	140.16		0.1	0.2	
7.24	C11-dicycloparaffin		$C_{11}H_{20}$	152.16		0.3	0.2	
7.29	alkyl benzene		$C_{10}H_{14}$	134.11	0.3	0.4		0.3
7.30	C11-paraffin		$C_{11}H_{24}$	156.19			0.5	
7.35	C11-paraffin		$C_{11}H_{24}$	156.19	0.2		0.6	
7.40	C11-monocycloparaffin		$C_{11}H_{22}$	154.17		0.2		
7.44	C11-paraffin		$C_{11}H_{24}$	156.19	0.4	0.6	1.7	
7.47	alkyl benzene		C_9H_{12}	120.09			0.4	0.3
7.49	benzene, (1-methylethyl)-	98-82-8	C_9H_{12}	120.09	0.9	1.2	0.7	1.0
7.51	C11-dicycloparaffin		$C_{11}H_{20}$	152.16				0.4
7.52	alkyl benzene		$C_{10}H_{14}$	134.11	0.5	0.6		
7.53	branched alkane						0.8	
7.63	C10-monocycloparaffin		$C_{10}H_{20}$	140.16	0.6	0.7	1.2	0.5
7.70	branched monocycloparaffin		$C_{11}H_{22}$	154.17	0.4	0.5	0.6	0.4
7.77	alkyl benzene		$C_{10}H_{14}$	134.11		0.2	0.2	
7.84	C11-monocycloparaffin		$C_{11}H_{22}$	154.17	0.3	0.3	0.2	0.3
7.91	alkyl benzene		$C_{10}H_{14}$	134.11	0.3	0.3	0.4	
7.94	benzene, 1-methyl-x-propyl-		$C_{10}H_{14}$	134.11	1.0	1.3	0.8	0.7
7.99	alkyl benzene		$C_{10}H_{14}$	134.11		0.9	1.1	0.5
8.00	C11-paraffin		$C_{11}H_{24}$	156.19	0.7			
8.02	naphthalene, decahydro-, trans	493-02-7	$C_{10}H_{18}$	138.14	0.9	0.9	0.4	0.8

8.05	benzene, x-ethyl-y,z-dimethyl-		$C_{10}H_{14}$	134.11	1.0	1.4	1.4	0.6
8.10	C11-paraffin		$C_{11}H_{24}$	156.19	0.6	0.6	1.1	0.4
8.21	alkyl benzene		$C_{10}H_{14}$	134.11	1.2	1.1	1.1	0.6
8.36	alkyl benzene		$C_{10}H_{14}$	134.11	1.0	0.8	0.4	0.7
8.39	alkyl benzene		$C_{10}H_{14}$	134.11	0.8	0.6	0.3	0.5
8.43	C11-monocycloparaffin		$C_{11}H_{22}$	154.17				
8.44	C11-monocycloparaffin		$C_{11}H_{22}$	154.17	0.3	0.6	0.4	0.3
8.49	alkyl benzene		$C_{10}H_{14}$	134.11	0.9	1.0	0.5	0.6
8.50	monocycloparaffin						0.3	
8.52	alkyl tetralin/indane		$C_{10}H_{12}$	132.09	0.6			0.8
8.53	C11-monocycloparaffin		$C_{11}H_{22}$	154.17		0.7	0.2	
8.60	alkyl benzene		$C_{11}H_{16}$	148.13	0.2	0.3	0.1	0.3
8.64	n-undecane	1120-21-4	$C_{11}H_{24}$	156.19	2.3	2.9	5.8	1.7
8.73	alkyl benzene		$C_{11}H_{16}$	148.13	0.3	0.5	0.3	0.4
8.77	alkyl benzene		$C_{11}H_{16}$	148.13	0.7	0.9	0.4	0.5
8.82	alkyl benzene		$C_{11}H_{16}$	148.13	0.6	0.6	0.3	0.6
8.87	alkyl benzene		$C_{11}H_{16}$	148.13			0.2	
8.90	decahydronaphthalene, trans-4a-methyl-	2547-27-5	$C_{11}H_{20}$	152.16	0.5	0.7	0.2	0.9
8.93	alkyl benzene		$C_{10}H_{14}$	134.11	0.6		0.5	0.5
8.93	C12-paraffin		$C_{12}H_{26}$	170.20			0.3	
8.96	alkyl benzene		$C_{10}H_{14}$	134.11	0.7	1.0	0.4	0.7
9.04	p-cymene	99-87-6	$C_{10}H_{14}$	134.11	0.9	1.3	0.5	0.7
9.09	C12-or C13-paraffin				0.4	0.4	0.6	0.4
9.16	decahydronaphthalene, x-methyl-		$C_{11}H_{20}$	152.16	0.6	0.9	0.3	1.3
9.24	C11-monocycloparaffin		$C_{11}H_{22}$	154.17	0.4	0.5	0.5	0.3
9.29	alkyl benzene		$C_{11}H_{16}$	148.13	0.6	0.6	0.3	0.6

9.34	alkyl indane/tetralin		$C_{11}H_{14}$	146.11	0.3	0.3		
9.34	C10-monocycloparaffin		$C_{10}H_{20}$	140.16			0.2	
9.35	C11-dicycloparaffin		$C_{11}H_{20}$	152.16				0.5
9.39	alkyl benzene		$C_{11}H_{16}$	148.13	0.9	0.9	0.3	0.9
9.43	mono- or di-cycloparaffin				0.2	0.3		**0.5**
9.49	C12-paraffin		$C_{12}H_{26}$	170.20		0.1	0.5	0.2
9.51	alkyl benzene		$C_{11}H_{16}$	148.13	1.5	1.5	0.7	1.3
9.54	alkyl benzene		$C_{10}H_{14}$	134.11	0.9	0.5		0.9
9.57	undecane, 4-methyl-	2980-69-0	$C_{12}H_{26}$	170.20	0.5	0.5	0.5	0.6
9.60	alkyl benzene		$C_{11}H_{16}$	148.13	0.7	0.5		0.6
9.64	C12-paraffin		$C_{12}H_{26}$	170.20		0.9	1.0	0.7
9.65	alkyl benzene		$C_{11}H_{16}$	148.13	1.2			
9.68	alkyl benzene		$C_{11}H_{16}$	148.13	0.3			
9.70	naphthalene, 1,2,3,4-tetrahydro-	119-64-2	$C_{10}H_{12}$	132.09	0.7		0.3	0.9
9.71	alkyl benzene		$C_{11}H_{16}$	148.13	0.4	0.5		
9.74	undecane, x-methyl-		$C_{12}H_{26}$	170.20	1.2		0.7	
9.74	C12-dicycloparaffin		$C_{12}H_{22}$	166.17		1.1		1.0
9.77	C12-dicycloparaffin		$C_{12}H_{22}$	166.17	0.3	0.3		0.4
9.82	paraffin						0.1	
9.86	benzene, 1-methyl-4-(1-methylpropyl)-	1595-16-0	$C_{11}H_{16}$	148.13	0.5	0.5	0.2	0.5
9.93	tricycloparaffin		$C_{12}H_{20}$	164.16	0.2	0.3	0.1	0.3
9.96	naphthalene, decahydro-x,y-dimethyl-		$C_{12}H_{22}$	166.17	0.5	0.4		0.8
10.00	branched benzene							0.6
10.00	C12-monocycloparaffin		$C_{12}H_{24}$	168.19	0.8	0.8		
10.01	C12-dicycloparaffin		$C_{12}H_{22}$	166.17			0.3	0.8
10.04	naphthalene	91-20-3	$C_{10}H_{8}$	128.06	0.6	0.8	0.2	0.5
10.08	alkyl tetralin/indane		$C_{11}H_{14}$	146.11	0.6			0.7

10.08	alkyl benzene		$C_{12}H_{18}$	162.14		0.6		
10.10	alkyl tetralin/indane		$C_{11}H_{14}$	146.11	0.4	0.7		0.6
10.14	alkyl benzene		$C_{12}H_{18}$	162.14	0.4			
10.14	monocycloparafin						0.4	
10.15	n-dodecane	112-40-3	$C_{12}H_{26}$	170.20	3.0	3.3	4.9	2.7
10.20	alkyl benzene		$C_{11}H_{14}$	146.11	0.4	0.5	0.2	0.5
10.24	alkyl tetralin/indane		$C_{11}H_{14}$	146.11	0.7	0.6		1.0
10.30	alkyl benzene		$C_{12}H_{18}$	162.14	0.3	0.4	0.2	0.3
10.35	undecane, 2,x-dimethyl-		$C_{13}H_{28}$	184.22	1.2	1.2	1.4	1.3
10.44	undecane, 2,x-dimethyl-		$C_{13}H_{28}$	184.22			0.3	
10.44	alkyl benzene		$C_{12}H_{18}$	162.14		0.3		
10.44	alkyl tetralin/indane		$C_{12}H_{16}$	160.12	0.3			0.5
10.49	alkyl tetralin/indane		$C_{11}H_{14}$	146.11	0.7	0.4		1.2
10.50	C13-paraffin		$C_{13}H_{28}$	184.22			0.4	
10.57	C13-monocylcoparaffin		$C_{13}H_{26}$	182.20	0.7	0.4	0.3	0.8
10.61	alkyl benzene		$C_{12}H_{18}$	162.14		0.7	0.3	
10.65	alkyl tetralin/indane		$C_{11}H_{14}$	146.11	0.4	0.3		
10.65	naphthalene, 1,2,3,4-tetrahydro-1-methyl-	1559-81-5	$C_{12}H_{22}$	166.17	0.2		0.2	0.7
10.71	C13-dicycloparaffin		$C_{13}H_{24}$	180.19	0.1	0.2		0.2
10.77	branched benzene		$C_{12}H_{18}$	162.14	1.0			0.9
10.78	C12-monocycloparaffin		$C_{12}H_{24}$	168.19		1.0	0.5	
10.82	branched benzene		$C_{12}H_{18}$	162.14	0.4	0.4		0.6
10.87	benzene, 1,4-dimethyl-2-(2-methylpropyl)-	55669-88-0	$C_{12}H_{18}$	162.14	0.6	0.4		0.5
10.90	C12-dicycloparaffin		$C_{12}H_{22}$	166.17				0.4
10.93	C13-monocycloparaffin		$C_{13}H_{26}$	182.20	0.5	0.4	0.4	0.5
10.96	C13-monocycloparaffin		$C_{13}H_{26}$	182.20			0.3	0.6

10.97	alkyl benzene		$C_{12}H_{18}$	162.14	0.6	0.5		
10.98	alkyl tetralin/indane		$C_{12}H_{16}$	160.12	0.5	0.4		0.6
10.99	C13-monocycloparaffin		$C_{13}H_{26}$	182.20			0.2	
11.02	dodecane, x-methyl		$C_{13}H_{28}$	184.22	0.7	0.5	0.4	0.5
11.09	dodecane, x-methyl		$C_{13}H_{28}$	184.22	1.1	0.9	0.7	0.8
11.14	C13-dicycloparaffin		$C_{13}H_{24}$	180.19	0.3			0.6
11.18	dodecane, x-methyl		$C_{13}H_{28}$	184.22	1.2	0.9	0.5	1.0
11.20	alkyl tetralin/indane		$C_{11}H_{14}$	146.11	1.4			2.3
11.21	C14-paraffin		$C_{14}H_{30}$	198.23		1.1	1.2	
11.31	C14-paraffin		$C_{14}H_{30}$	198.23			0.2	
11.31	alkyl benzene		$C_{12}H_{18}$	162.14	0.4	0.2		
11.34	alkyl benzene		$C_{12}H_{18}$	162.14	0.5	0.4		
11.38	C14-monocycloparafin		$C_{14}H_{28}$	196.22	0.2		0.2	0.4
11.42	alkyl benzene		$C_{12}H_{18}$	162.14	0.6	0.5	0.1	0.7
11.48	cyclotridecane	295-02-3	$C_{13}H_{26}$	182.20	0.4	0.5		0.3
11.49	monocycloparaffin						0.2	
11.50	alkyl tetralin/indane		$C_{12}H_{16}$	160.12	0.3			0.3
11.59	n-tridecane	629-50-5	$C_{13}H_{28}$	184.22	2.9	3.0	3.9	2.8
11.60	alkyl tetralin/indane		$C_{11}H_{14}$	146.11				1.6
11.64	naphthalene, x-methyl-		$C_{11}H_{10}$	142.08	1.3	1.8	0.6	1.1
11.74	alkyl tetralin/indane		$C_{12}H_{16}$	160.12	0.5	0.4	0.4	0.6
11.77	dicycloparaffin		$C_{13}H_{26}$	182.20	0.2	0.2		0.3
11.85	C14-paraffin		$C_{14}H_{30}$	198.23	0.4	0.4	0.4	0.5
11.89	naphthalene, x-methyl-		$C_{11}H_{10}$	142.08	0.5	0.9	0.2	0.5
11.92	alkyl benzene		$C_{13}H_{20}$	176.16		0.5		0.3
11.93	naphthalene, 1,2,3,4-tetrahydro-2,3-dimethyl-	21564-92-1	$C_{12}H_{16}$	160.12	1.1			1.8

12.02	alkyl indane/tetralin		$C_{13}H_{18}$	174.14	0.3			0.6
12.05	paraffin							0.3
12.06	C13-dicycloparaffin		$C_{13}H_{24}$	180.19		0.3		
12.07	alkyl indane/tetralin		$C_{13}H_{18}$	174.14	0.4	0.2		0.6
12.10	alkyl benzene		$C_{12}H_{16}$	160.10			0.1	0.3
12.14	alkyl indane/tetralin		$C_{13}H_{18}$	174.14	0.2	0.1		
12.20	C14-monocycloparaffin		$C_{14}H_{28}$	196.22				0.7
12.23	heptylcyclohexane	5617-41-4	$C_{13}H_{26}$	182.20	0.7	0.7	0.4	
12.28	alkyl indane/tetralin		$C_{13}H_{18}$	174.14	0.5			1.1
12.29	tridecane, 6-methyl-	13287-21-3	$C_{14}H_{30}$	198.23		0.4	0.3	
12.33	alkyl indane/tetralin		$C_{12}H_{16}$	160.12	0.8			1.1
12.33	tridecane, 5-methyl-	25117-31-1	$C_{14}H_{30}$	198.23		0.3	0.3	
12.39	tridecane, 4-methyl-	26730-12-1	$C_{14}H_{30}$	198.23	0.5	0.4	0.4	0.4
12.45	tridecane, x-methyl-		$C_{14}H_{30}$	198.23	0.6	0.6	0.5	0.5
12.46	cyclohexane, (2,2-dimethylcyclopentyl)-	61142-23-2	$C_{13}H_{24}$	180.19				0.4
12.50	alkyl indane/tetralin		$C_{13}H_{18}$	174.14	0.5			0.4
12.50	alkyl benzene		$C_{13}H_{20}$	176.16		0.2		
12.55	tridecane, x-methyl-		$C_{14}H_{30}$	198.23	0.5	0.4	0.4	0.4
12.59	alkyl benzene		$C_{13}H_{20}$	176.16	0.3	0.2		
12.63	hexadecane, 2,6,10,14-tetramethyl-	638-36-8	$C_{15}H_{32}$	212.25	0.7	0.7	0.8	0.9
12.72	alkyl indane/tetralin		$C_{14}H_{20}$	188.16	0.3	0.2		0.5
12.79	acenaphthene	83-32-9	$C_{11}H_{22}$	154.17	0.3	0.3		0.5
12.85	C15-monocycloparaffin		$C_{15}H_{30}$	210.23	0.3			0.4
12.89	n-tetradecane	629-59-4	$C_{14}H_{30}$	198.23	2.3	2.2	2.6	2.3
12.95	alkyl indane/tetralin		$C_{12}H_{16}$	160.12	0.6	0.4		0.9
13.01	C15-paraffin		$C_{15}H_{32}$	212.25	0.4	0.2	0.2	

13.08	naphthalene, 1,x-dimethyl		$C_{12}H_{12}$	156.09	0.2	0.2		0.3
13.13	naphthalene, 1,x-dimethyl		$C_{12}H_{12}$	156.09	0.7	1.2	0.4	0.6
13.28	alkyl benzene		$C_{14}H_{22}$	190.17	0.2			0.2
13.33	naphthalene, 1,x-dimethyl		$C_{12}H_{12}$	156.09	0.8	0.7	0.2	0.7
13.38	naphthalene, 1,x-dimethyl		$C_{12}H_{12}$	156.09	0.8	0.8	0.2	0.9
13.41	C15-dicycloparaffin		$C_{15}H_{28}$	208.22				0.4
13.44	alkyl indane/tetralin/benzene				0.3			0.3
13.45					0.2			
13.49	alkyl indane/tetralin				0.3			
13.54	alkyl indane/tetralin		$C_{14}H_{18}$	186.14	0.3	0.1		0.3
13.57	monocycloparffin		$C_{14}H_{28}$	196.22	0.5	0.5		
13.60	alkyl indane/tetralin		$C_{14}H_{20}$	188.16			0.4	0.6
13.63	naphthalene, x,y-dimethyl-		$C_{12}H_{12}$	156.09	0.4	0.2	0.1	
13.63	paraffin				0.3			
13.65	alkyl benzene		$C_{14}H_{22}$	190.17	0.4			0.4
13.76	C16-paraffin		$C_{16}H_{34}$	226.27	0.9	0.8	0.6	0.9
13.79	naphthalene, 1,x-dimethyl		$C_{12}H_{12}$	156.09	0.2	0.2		0.3
13.84	alkyl benzene		$C_{14}H_{22}$	190.17	0.4			0.3
13.84	C16-paraffin		$C_{16}H_{34}$	226.27		0.2		
13.88	decahydro-4,4,8,9,10-pentamethylnaphthalene	80655-44-3	$C_{15}H_{28}$	208.22	0.2	0.1		0.3
13.92	alkyl benzene		$C_{14}H_{22}$	190.17	0.2	0.1		0.2
13.97	hexadecane, 5-butyl-	6912-07-8	$C_{20}H_{42}$	282.33	0.2	0.1		0.4
14.00	branched benzene		$C_{14}H_{22}$	190.17	0.2			0.2
14.15	1,1'-biphenyl, x-methyl-		$C_{13}H_{12}$	168.09	0.2	0.2		0.4
14.15	n-pentadecane	629-62-9	$C_{15}H_{32}$	212.25	1.6	1.2	1.3	1.2
14.26	1,1'-biphenyl, x-methyl-		$C_{13}H_{12}$	168.09	0.1		0.1	0.3

14.32	paraffin				0.2			0.1
14.40	alkyl naphthalene		$C_{13}H_{14}$	170.11	0.2	0.1		0.3
14.50	alkyl naphthalene		$C_{13}H_{14}$	170.11	0.1	0.1		0.1
14.67	alkyl naphthalene		$C_{13}H_{14}$	170.11	0.3	0.3		0.2
14.73	alkyl naphthalene		$C_{13}H_{14}$	170.11	0.3	0.3		0.1
14.93	alkyl naphthalene		$C_{13}H_{14}$	170.11	0.2	0.2		0.1
14.96	alkyl naphthalene		$C_{13}H_{14}$	170.11	0.3			
15.06					0.2	0.1		
15.46	n-hexadecane	544-76-3	$C_{16}H_{34}$	226.27	0.7	0.6	0.3	0.2
15.96	paraffin				0.1	0.1		
16.50	n-heptadecane	629-78-7	$C_{17}H_{36}$	240.28	0.2	0.2		
16.60	paraffin				0.1	0.1		

Table 3. A comparison of the integral values for ^{1}H spectral regions for all of the neat gas turbine fuels Jet A-10325, JP-8-10264, and JP-5-10289.

ν (ppm)	**Proton Type**	**Jet A-10325 (mole % ^{1}H)**	**JP-8-10264 (mole % ^{1}H)**	**JP-5-10289 (mole % ^{1}H)**	**Rel. Uncertainty[c] (%)**
10.7 - 7.4	polyaromatic CH	0.53	2.96	0.30	7.1
7.4 - 6.2	monoaromatic CH	2.89	5.24	2.88	1.5
6.2 - 5.1	olefinic CH	[b]	[b]	[b]	-
5.1 - 4.3	olefinic CH_2	[b]	[b]	[b]	-
4.3 - 2.4 [a]	α-to-aromatic CH_2	3.19	2.63	3.54	6.6
2.4 - 2.1	α-to-aromatic CH_3	4.02	3.75	3.78	2.1
2.0 - 1.02	paraffinic CH_2	55.23	55.85	54.11	0.9
1.02 - 0.2	paraffinic CH_3	34.14	35.12	35.39	1.3

[a] The water signal at ~2.8 ppm was excluded from the integral.
[b] The integral value was ≤0.02 %, which is the detection limit.
[c] This is the relative combined standard uncertainty in the integral values.

Table 4. A comparison of the integral values for ^{13}C spectral regions for all of the neat gas turbine fuels Jet A-10325, JP-8-10264, and JP-5-10289.

ν (ppm)	**Carbon Type**	**Jet A-10325 (mole % ^{13}C)**	**JP-8-10264 (mole % ^{13}C)**	**JP-5-10289 (mole % ^{13}C)**	**Rel. Uncertainty [b] (%)**
170 - 131.2	quaternary aromatic	4.23	2.96	4.11	14.5
131.2 - 115.5	aromatic CH	6.48	5.24	5.80	8.8
115.5 - 100	olefin	[a]	[a]	[a]	-
70.0 - 45.0	paraffinic CH	1.76	0.80	4.13	24.9
45.0 - 32.7	paraffinic CH & CH_2	18.86	17.56	23.48	4.6
32.7 - 30.8	chain γ-CH_2, β to aromatic CH_2	9.69	10.57	8.84	3.7
30.8 - 28.5	chain δ-CH_2, α to aromatic naphthenes, aromatic attached ethyl CH_2	16.27	19.05	13.72	2.2
28.5 - 25.0	cycloparaffin CH_2	8.27	8.03	8.33	3.0
25.0 - 21.9	chain β-CH_2, α to ring CH_3	12.09	14.34	10.65	2.1
21.9 - 17.6	α to ring CH_3	9.98	8.71	10.26	4.3
17.6 - 14.7	aromatic-attached ethyl CH_3	1.37	0.82	1.84	8.7
14.7 - 12.3	chain α-CH_3	8.71	9.79	6.88	2.7
12.3 - 0.0	branched-chain CH_3	2.31	1.98	1.97	13.9

[a] The integral value was ≤0.02 %, which is the detection limit.
[b] This is the relative combined standard uncertainty in the integral values.

Table 5. A summary of the average boiling behavior of the gas turbine fuels as measured by T_k. The vapor rise temperature is that at which vapor is observed to rise into the distillation head, considered to be the initial boiling point (IBT) of the fluid (highlighted in bold print). These temperatures have been adjusted to 1 atmosphere with the modified Sydney Young equation; the average experimental atmospheric pressures are provided to allow recovery of the average measured temperatures. The uncertainties are discussed in the text.

Samples	Average Pressure (kPa)	Sustained Boiling Temperature (°C)	Vapor Rise Temperature (°C)
Jet A-10325	83.1	179.8	**186.1**
JP-8-10264	83.2	166.0	**173.1**
JP-5-10289	83.6	195.6	**203.0**

Table 6. Representative distillation curve data (given as the average of three distillation curves) for gas turbine fuels. These temperatures in the kettle and in the head (T_k and T_h, respectively) have been adjusted to 1 atm with the modified Sydney Young equation; the average experimental atmospheric pressures are provided to allow recovery of the actual average measured temperatures. The uncertainties are discussed in the text.

	Jet A-10325 83.1 kPa		**JP-8-10264 83.2 kPa**		**JP-5-10289 83.6 kPa**	
DVF (%)	T_k (°C)	T_h (°C)	T_k (°C))	T_h (°C)	T_k (°C)	T_h (°C)
5	190.4	175.0	176.5	168.2	206.7	198.0
10	193.7	180.3	179.4	171.8	209.6	202.0
15	196.7	184.5	181.9	174.8	212.3	205.4
20	199.6	188.2	184.4	177.4	215.2	208.7
25	202.4	191.1	187.0	180.2	217.6	211.3
30	205.5	194.5	189.5	183.2	220.2	214.3
35	208.2	198.4	192.3	186.2	222.4	217.0
40	211.0	201.3	195.1	188.9	224.8	219.4
45	214.4	204.7	198.4	192.7	227.0	222.2
50	217.4	207.9	201.9	196.2	229.3	224.8
55	220.7	211.8	205.2	199.4	231.3	227.5
60	224.7	216.1	209.5	204.0	233.7	230.3
65	228.6	220.2	214.2	208.7	236.3	232.9
70	233.0	224.5	219.2	214.1	238.9	236.3
75	237.6	229.3	224.8	219.8	241.6	239.7
80	242.7	234.5	231.7	226.8	245.3	243.3
85	246.1	241.4	238.5	234.1	248.5	247.2
90	255.2	248.1	244.3	243.2	253.0	252.6

Table 7. Table of the hydrocarbon family types resulting from a mass spectrometric classification technique, similar to ASTM D-2789, performed on the neat samples of the gas turbine fuels Jet A-10325, JP-8-10264, and JP-5-10289.

Sample	**Paraffins (%)**	**Monocycloparaffins (%)**	**Dicycloparaffins (%)**	**Alkylbenzenes (%)**	**Indanes and Tetralins (%)**	**Naphthalenes (%)**
Jet A-10325	38.8	26.9	11.2	16.1	3.7	3.3
JP-8-10264	49.3	25.2	7.7	12.8	2.4	3.9
JP-5-10289	28.6	27.9	17.0	15.3	8.4	2.8

Table 8. Energy content, presented as the composite enthalpy of combustion – ΔH_c (kJ/mol), as a function of the distillate volume fraction for each gas turbine fuels Jet A-10325, JP-8-10264, and JP-5-10289. The uncertainties are discussed in the text and are provided in parentheses.

Composite Enthalpy of Combustion, kJ/mol									
Sample	*0.03%*	*10%*	*20%*	*30%*	*40%*	*50%*	*60%*	*70%*	*80%*
Jet A-10325	5119 (512)	5728 (286)	5996 (300)	6252 (313)	6547 (360)	6771 (339)	7113 (356)	7652 (383)	8019 (401)
JP-8-10264	5268 (526)	5690 (285)	5881 (294)	6102 (305)	6275 (314)	6473 (324)	6693 (335)	7155 (358)	7657 (383)
JP-5-10289	5447 (545)	6059 (303)	6727 (336)	7038 (352)	7198 (360)	7438 (372)	7625 (381)	7949 (397)	8219 (411)

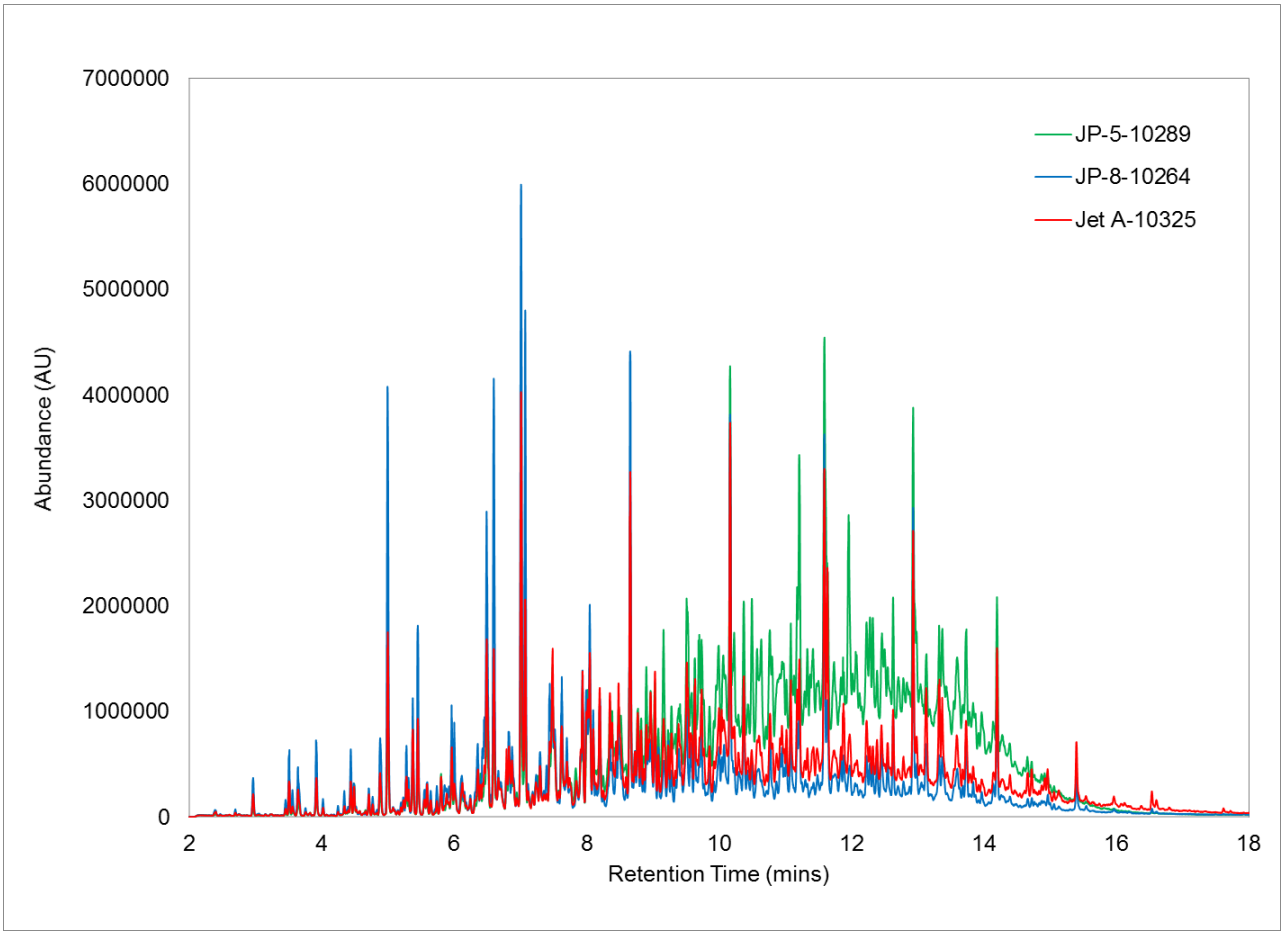

Figure 1. A chromatogram of the abundance of mass fragment ions as a function of acquisition time is presented for Jet A-10325 (red line), JP-8-10264 (blue line), and JP-5-10289 (green line) analyzed with GC/QTOF-MS as described in the experimental section.

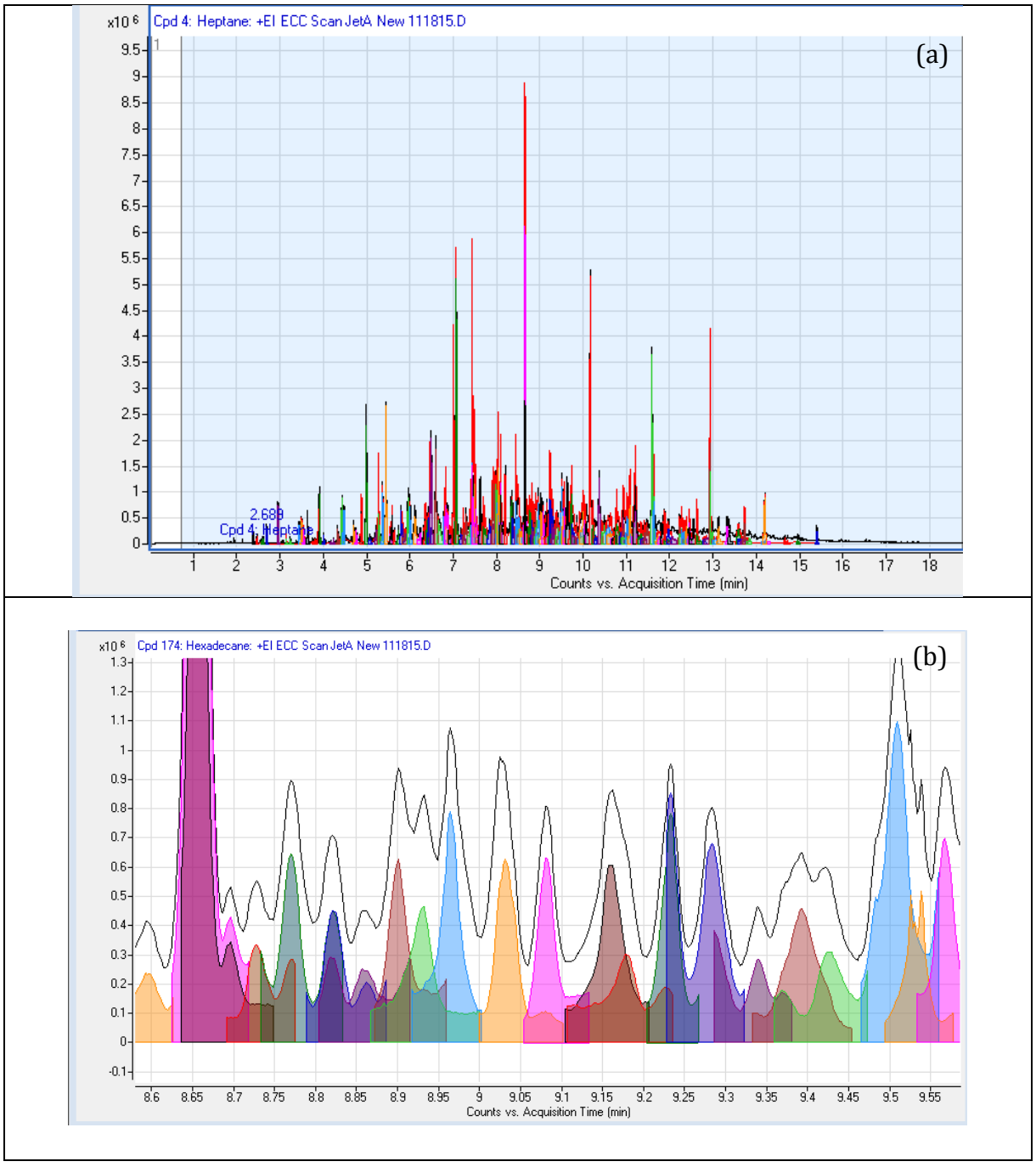

Figure 2. The results of the deconvolution algorithm as applied to the Jet-A-10325 chromatogram is presented for both the full chromatogram (a) and a zoomed-in section of one minute retention time (b).

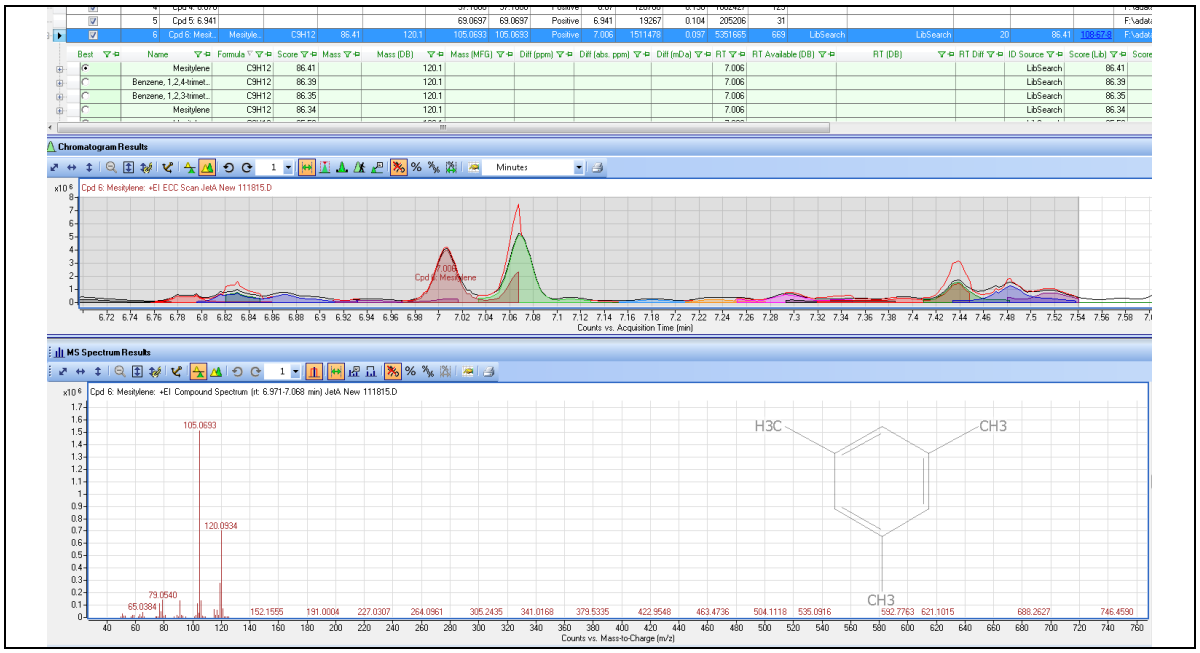

Figure 3. The output from the analysis program showing an example of a peak at 7.006 mins, identified as 1,3,5-trimethylbenzene. The analysis program used the NIST/EPA/NIH Mass Spectral Database released in 2011 to select the ten most-likely candidates for each resolved peak. The GC/QTOF-MS experimentally determined this compounds m/z to be 120.0934, which is the exact calculated theoretical mass for this compound's radical cation.

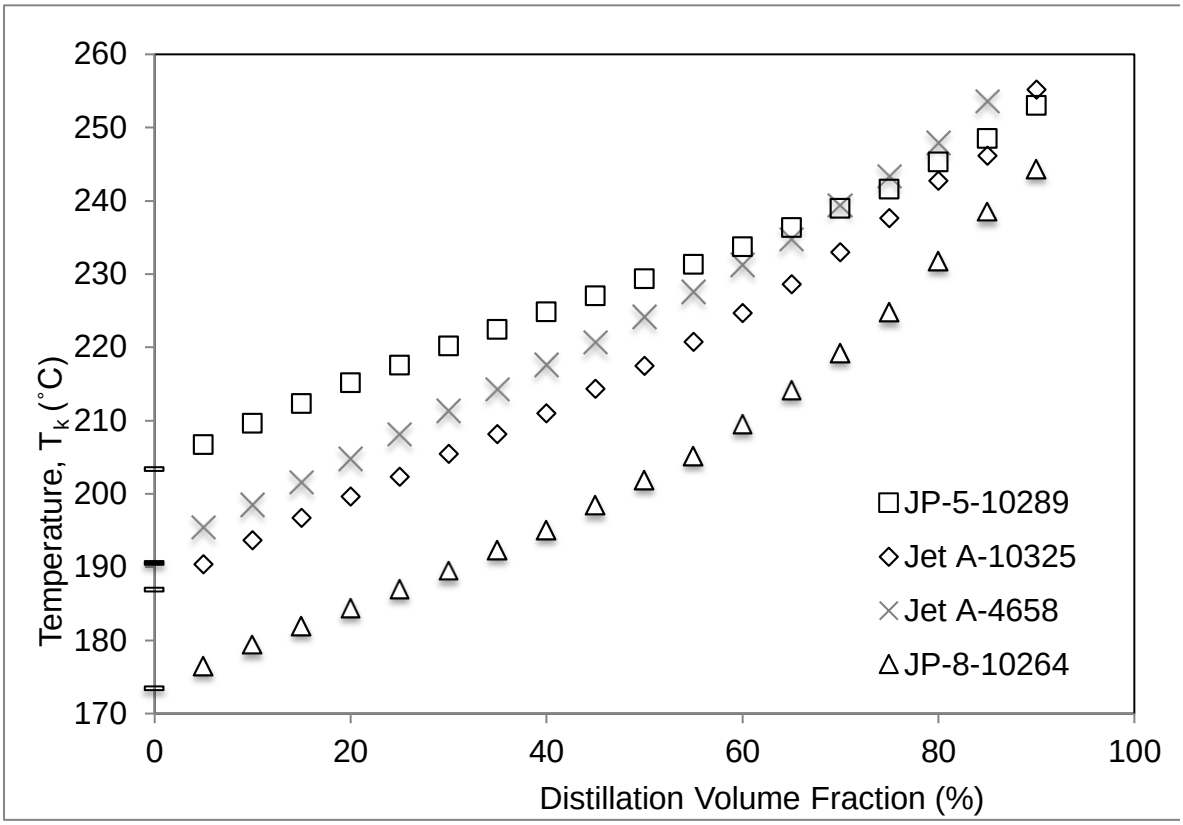

Figure 4. Distillation curves for the gas turbine fuels Jet A-10325, JP-8-10264, JP-5-10289, and the previously measured Jet A-4658.[24] The symbols on the y-axis are the temperatures at which the first drop falls into the level-stabilized receiver. The first drop is considered the 0.025 % distillate volume fraction.The uncertainties are discussed in the text.

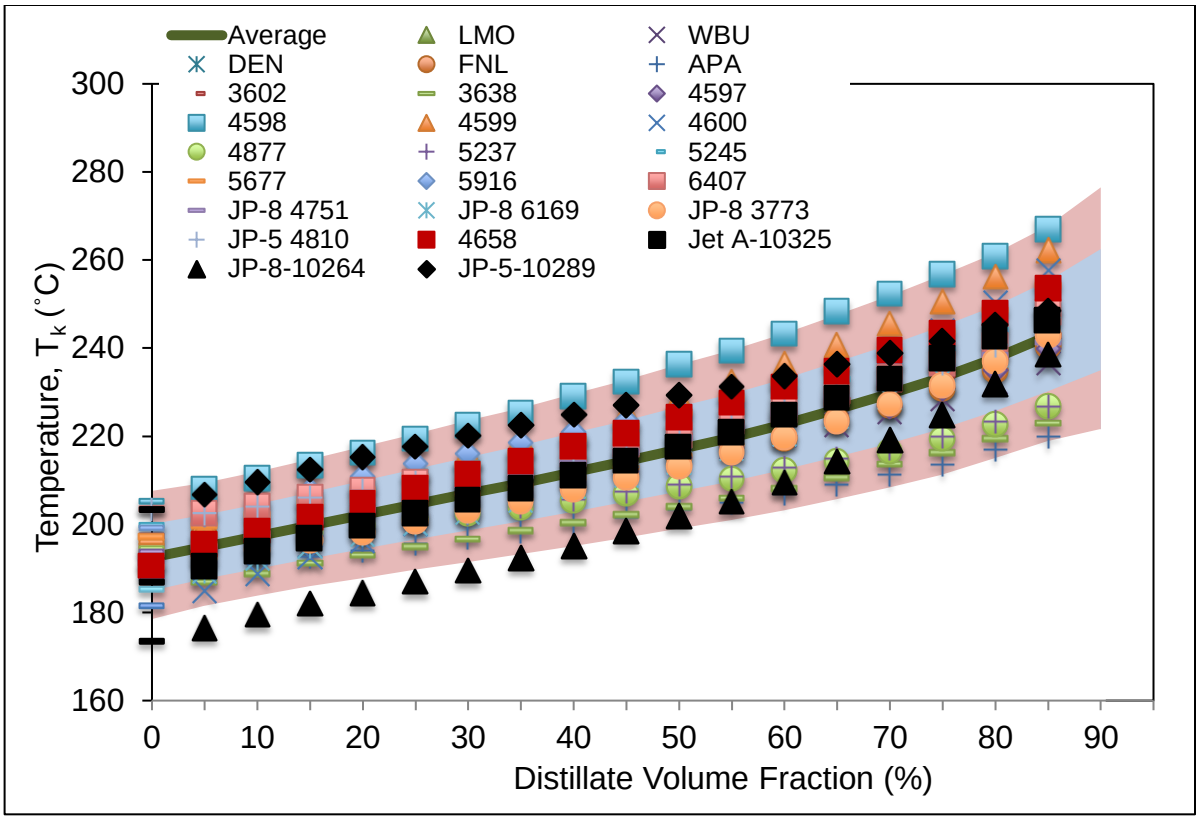

Figure 5. Distillation curves for the gas turbine fuels Jet A-10325 (black squares), JP-8-10264 (black triangles), and JP-5-10289 (black diamonds) presented along with the eighteen previously measured gas turbine fuels.[24] The shaded areas in blue and pink represent one and two standard deviation respectively from the average distillation temperatures (solid line) of all 21 fuels measured in our laboratory. The uncertainties are discussed in the text.

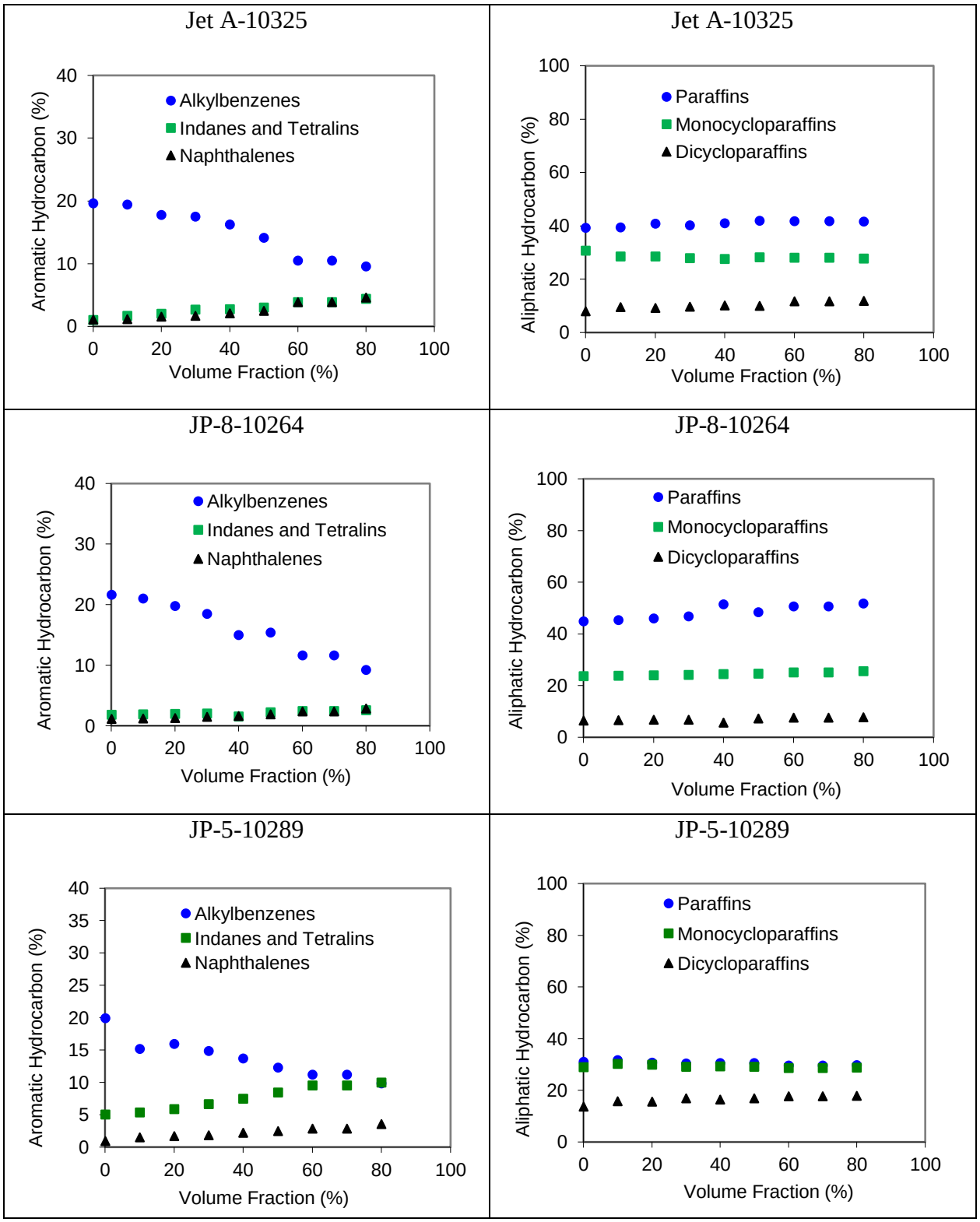

Figure 6. Plots of the hydrocarbon family types resulting from the moiety family analysis performed on gas turbine fuels Jet A-10325, JP-8-10264, and JP-5-10289 obtained from a mass spectrometric fragment classification technique, similar to ASTM D-2789. The uncertainty is discussed in the text.

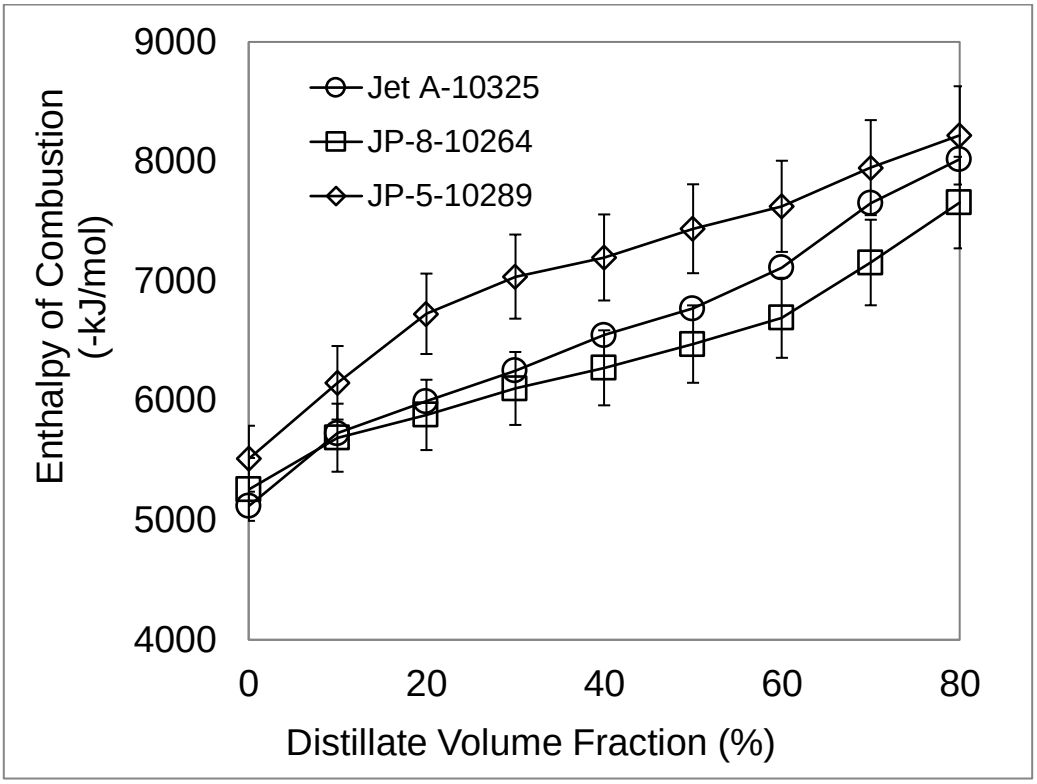

Figure 7. Energy content, presented as the composite enthalpy of combustion, $-\Delta H_c$ (kJ/mol), as a function of the distillate volume fraction for gas turbine fuels Jet A-10325, JP-8-10264, and JP-5-10289. The uncertainties are discussed in the text. Lines are drawn to guide the eyes of the viewer, and do not represent a fit.